Received: 23 February 2023 | Revised: 19 May 2023 | Accepted: 12 June 2023

DOI: 10.1002/alz.13385

Alzheimer's & Dementia®
THE JOURNAL OF THE ALZHEIMER'S ASSOCIATION

RESEARCH ARTICLE

FDG-PET markers of heterogeneity and different risk of progression in amnestic MCI

Silvia Paola Caminiti[1,2] | **Silvia De Francesco**[3] | **Giacomo Tondo**[1,2] | **Alice Galli**[1,2] | **Alberto Redolfi**[3] | **Daniela Perani**[1,2] | **the Alzheimer's Disease Neuroimaging Initiative** | **the Interceptor Project**

[1]Vita-Salute San Raffaele University, Milan, Italy

[2]Division of Neuroscience, IRCCS San Raffaele Scientific Institute, Milan, Italy

[3]Laboratory of Neuroinformatics, IRCCS Istituto Centro San Giovanni di Dio Fatebenefratelli, Brescia, Italy

Correspondence
Daniela Perani, Vita-Salute San Raffaele University, Nuclear Medicine Unit San Raffaele Hospital, Division of Neuroscience, San Raffaele Scientific Institute, Via Olgettina 60, 20132 Milan, Italy.
Email: perani.daniela@hsr.it

Part of the data used in the preparation of this article were obtained from the Alzheimer's Disease Neuroimaging Initiative (ADNI) database (adni.loni.usc.edu). The investigators of the ADNI contributed to the design and implementation of the ADNI and/or provided data, but they did not participate in the analysis or writing of this report. A complete list of the ADNI investigators can be found at http://adni.loni.usc.edu/wpcontent/uploads/how_to_apply/ADNI_Acknowledgement_List.pdf

Part of the data used in the preparation of this article were obtained from The Interceptor Project. The Interceptor Coordinator Group: Stefano F. Cappa, ICoN Cognitive Neuroscience Center, IUSS, Institute for Advanced Studies and IRCCS Mondino Foundation, 27100 Pavia, Italy; Maria Cotelli, Neuropsychology Unit, IRCCS Istituto Centro San Giovanni di Dio Fatebenefratelli, 25125 Brescia, Italy; Camillo Marra, Neurology Unit, Fondazione Policlinico Universitario "A. Gemelli" IRCCS, 00168 Rome, Italy; Paolo Maria Rossini, Dept. Neurosci. & Neurorehab., IRCCS San Raffaele-Roma, 00163 Rome, Italy; Patrizia Spadin, President "Associazione

Abstract

INTRODUCTION: Amnestic mild cognitive impairment (aMCI) is emerging as a heterogeneous condition.

METHODS: We looked at a cohort of $N = 207$ aMCI subjects, with baseline fluorodeoxyglucose positron emission tomography (FDG-PET), T1 magnetic resonance imaging, cerebrospinal fluid (CSF), apolipoprotein E (*APOE*), and neuropsychological assessment. An algorithm based on FDG-PET hypometabolism classified each subject into subtypes, then compared biomarker measures and clinical progression.

RESULTS: Three subtypes emerged: hippocampal sparing–cortical hypometabolism, associated with younger age and the highest level of Alzheimer's disease (AD)-CSF pathology; hippocampal/cortical hypometabolism, associated with a high percentage of *APOE* ε3/ε4 or ε4/ε4 carriers; medial–temporal hypometabolism, characterized by older age, the lowest AD-CSF pathology, the most severe hippocampal atrophy, and a benign course. Within the whole cohort, the severity of temporo-parietal hypometabolism, correlated with AD-CSF pathology and marked the rate of progression of cognitive decline.

DISCUSSION: FDG-PET can distinguish clinically comparable aMCI at single-subject level with different risk of progression to AD dementia or stability. The obtained results can be useful for the optimization of pharmacological trials and automated-classification models.

KEYWORDS
amnestic, biomarker, dementia, hypometabolism, neurodegeneration

Italiana Malattia di Alzheimer" – AIMA, Italy; Fabrizio Tagliavini, Fondazione IRCCS Istituto Neurologico "Carlo Besta," 20133 Milano, Italy; Nicola Vanacore, National Center for Disease Prevention and Health Promotion, National Institute of Health, Rome, Italy; Fabrizio Vecchio, Brain Connectivity Laboratory, Department of Neuroscience and Neurorehabilitation, IRCCS San Raffaele Roma, 00163 Rome, Italy.

Funding information
Italian Ministry of Health; Italian Medicines Agency (AIFA)

Highlights

- Algorithm based on FDG-PET hypometabolism demonstrates distinct subtypes across aMCI;
- Three different subtypes show heterogeneous biological profiles and risk of progression;
- The cortical hypometabolism is associated with AD pathology and cognitive decline;
- MTL hypometabolism is associated with the lowest conversion rate and CSF-AD pathology.

1 | BACKGROUND

Amnestic mild cognitive impairment (aMCI) is considered the most common presentation of Alzheimer's disease (AD) because a considerable portion of people with aMCI will ultimately convert to AD over 2 to 5 years.[1] Clinical trials have thus generally considered aMCI as a model of typical prodromal AD.[2] However, not all aMCI subjects belong to the AD spectrum or convert to dementia. A substantial number of aMCI subjects have mixed pathologies or primary pathologies other than AD.[3] Of note, some aMCI subjects show an unusually long-lasting course with no or a very slow rate of cognitive decline.[4] The use of biomarkers can help to characterize the underlying disease, providing better diagnosis and prognosis in clinical settings, mandatory for the proper inclusion in disease-modifying treatments.

AD is biologically defined by biomarkers of amyloid beta (Aβ) plaques, neurofibrillary tau tangles (NFT) in the brain, and neurodegeneration.[5] However, both Aβ plaques and NFT are frequently present in other brain conditions or observed as co-pathology in *post mortem* examination of people who had other neurodegenerative diseases.[6] In these situations, pathophysiological AD biomarkers can be positive, and this biomarker positivity is ambiguous, particularly in the asymptomatic individuals and in the earliest disease phases.[7,8] Among the AD Aβ positive individuals, neuropathology and neuroimaging data point out the existence of heterogeneity in atrophy, and amyloid and tau distribution (see Ferreira et al.[9] for a meta-analysis). The emerging tau positron emission tomography (PET) biological subtypes in particular, indicate interindividual differences in clinical presentations and cognitive trajectories.[10] Tau PET imaging is in addition not widely available, and further research work is necessary to consolidate its diagnostic accuracy in AD and other dementia conditions.[11] Tau pathology correlates with neuronal and synaptic loss,[12] which is also detectable by ^{18}F-fluorodeoxyglucose (FDG)-PET brain metabolism.[13] FDG-PET is a widely available technique providing information on the distribution of neuronal synapse dysfunction and is more sensitive than magnetic resonance imaging (MRI) structural information to detect early neurodegenerative processes.[14,15] Specific hypometabolic patterns support differential diagnosis in AD, frontotemporal dementia spectrum, and atypical parkinsonian disorders.[16] The high diagnostic power of FDG-PET imaging is also accompanied by a relatively low cost, and availability of validated and standardized analytic procedures. Recently, FDG-PET brain metabolism was incorporated in artificial intelligence (AI) emerging pipelines for neurodegenerative diseases, showing clear-cut evidence of its specific diagnostic role.[17] Its importance in the preclinical/prodromal phase is becoming more and more relevant, considering the accuracy in detecting brain dysfunctional changes well before the structural MRI evidence,[18,19] and the need for highly accurate framing of prodromal subjects who will be chosen for inclusion in disease-modifying drug trials.

The characterization of FDG-PET hypometabolism in aMCI is still controversial. Some studies report that parieto-temporal hypometabolism, and especially in the posterior cingulate cortex (PCC), without medial temporal lobe (MTL) involvement, is the most characteristic FDG pattern in aMCI[20,21] predicting progression to AD dementia.[22] Other studies identified the MTL hypometabolism as the earliest typical pattern associated with the amnestic onset in MCI due to AD.[23,24] However, the presence in the aMCI clinical phenotype of focal hypometabolism in the MTL structures, accompanied by negative or variable amyloid load and a clinical benign course over long follow-up periods, has been reported in association with non-AD pathological substrates.[25–27]

No studies yet have systematically assessed FDG-PET hypometabolism patterns in terms of spatial distribution and severity in a clinically comparable large group of aMCI subjects, also considering the prognostic value. We used an algorithm based on FDG-PET to describe the different expression of cortical and MTL hypometabolism in a large cohort of aMCI subjects studied in terms of key demographic, clinical, apolipoprotein E (*APOE*) genotyping, cerebrospinal fluid (CSF), and MRI measures. The predictive value of the subtypes was tested in a subgroup of aMCI with available follow-up information.

2 | METHODS

2.1 | Subjects

aMCI subjects were retrospectively included from the Italian INTERCEPTOR project (aMCI-INTERCEPTOR cohort), and the Alzheimer's Disease Neuroimaging Initiative (ADNI) database, screening the ADNI-1, ADNI-GO, and ADNI-2 phases (aMCI-ADNI cohort). For up-to-date

information see https://adni.loni.usc.edu. The Italian INTERCEPTOR project, promoted by the Italian Medicines Agency and the Italian Ministry of Health (https://www.interceptorproject.com/en/) is a multicenter, interventional, non-therapeutic cohort study in subjects with MCI.[28]

Inclusion criteria were: (1) aMCI diagnosis according to Petersen criteria;[29] (2) FDG-PET scan performed at baseline and analyzed using the optimized statistical parametric mapping (SPM) procedure[30,31] showing brain hypometabolism in the typical AD-like structures, namely the hippocampal structures and/or the temporo-parietal associative cortex; (3) only for the aMCI-ADNI cohort, the presence of a follow-up clinical assessment ≥2 years.

Each subject also underwent a CSF exam, structural MRI, and *APOE* genotyping. The Mini-Mental State Examination (MMSE), Clinical Dementia Rating (CDR) scale, Neuropsychiatric Inventory (NPI), and standard neuropsychological batteries were administered. The autonomy in activities of daily living through the Functional Assessment Questionnaire (FAQ) and Instrumental Activities of Daily Living (IADL) were available at baseline. We included all aMCI subjects without requiring positive Aβ status. This is relevant because in clinical practice, most MCI subjects with amnestic onset have an unknown Aβ status.

The final whole sample consisted of a total of 207 individuals.

RESEARCH IN CONTEXT

1. **Systematic review**: The authors reviewed the literature using traditional (e.g., PubMed) sources and meeting abstracts and presentations. While amnestic mild cognitive impairment (aMCI) is considered the prodromal phase of Alzheimer's disease (AD), biomarker and clinical prospective evidence suggested a heterogeneous condition. These relevant citations are appropriately cited.
2. **Interpretation**: Here, in a large sample of MCI subjects with a comparable amnestic phenotype at baseline and no differences in global functioning, we distinguished three different subtypes, based on brain hypometabolism features. Each subject within the three subtypes showed a related set of biological features and distinct clinical trajectories, namely stability or rapid progression to dementia.
3. **Future directions**: Capturing this heterogeneity is crucial for diagnosis and prognosis, supporting the presence of AD and non-AD subtypes with different risk of progression that is a mandatory knowledge in disease-modifying treatments.

2.2 | FDG-PET procedures

The aMCI-INTERCEPTOR subjects underwent FDG-PET scan according to the conventional neurological acquisition protocols. See Rossini et al.[28] for further details about INTERCEPTOR acquisition procedures.

ADNI acquisition procedures are detailed in the ADNI PET Technical Procedures Manual, version 9.5 (https://adni.loni.usc.edu/methods/pet-analysis-method/pet-analysis/). For the aMCI-ADNI, the last three 5-minute frames of FDG-PET images were combined to obtain a single 15-minute static image, ensuring uniform acquisition procedures for all FDG-PET images, independent of the acquisition site.[32] A visual quality check of the images was performed to identify potential artifacts.

Then, FDG-PET images of patients were pre-processed using SPM12 (https://www.fil.ion.ucl.ac.uk/spm/) according to the validated pipeline proposed for the single-subject SPM-based analysis[30,31] (Figure 1).

A nuclear medicine expert blinded to any clinical information selected those aMCI with evidence of limbic and/or temporo-parietal hypometabolism.

The SPM-t hypometabolism maps were converted into the normal *z*-like distribution (SPM-z maps) with MATLAB R2021b (Mathworks Inc.). Low *z*-scores (<0) indicated more severe regional hypometabolism compared to healthy controls (HC).

2.3 | MRI procedures

Structural 3D MRIs (1.5 or 3 Tesla T1-weighted magnetization prepared rapid acquisition with gradient echo [MPRAGE] or inversion recovery fast spoiled gradient recalled [IR-FSPGR]) from Siemens, Philips, and GE scanners were included.

Preprocessing included registration through an affine transformation with 12 degrees of freedom to the Montreal Neurological Institute (MNI) MNI152 template (voxel size 1×1×1 mm). All scans were processed to correct for low frequency nonuniform intensities using Advanced Normalization Tools (ANTs).[33] MRI analysis was run in the neuGRID platform (https://neugrid2.eu),[34] an online high-performance computing infrastructure.

Based on the validated reference control group, consisting of 382 HC, we estimated atrophy *z*-score maps for the cortical and subcortical areas of interest obtained with FreeSurfer v. 7.1.1. Lower *z*-scores (<0) indicated greater regional atrophy compared to HC.

2.4 | FDG-PET subtype classification

2.4.1 | Structural atlas construction

Anatomical segmentation of a complete set of cortical and subcortical gray matter structures was performed with FreeSurfer v. 7.1.1 (Figure 1), using the cross-sectional stream via the recon-all script. FreeSurfer (http://surfer.nmr.mgh.harvard.edu/) segmentation includes (1) motion correction and averaging of multiple images when available; (2) removal of non-brain tissue; (3) Talairach transformation; (4) segmentation of subcortical white matter and deep gray matter

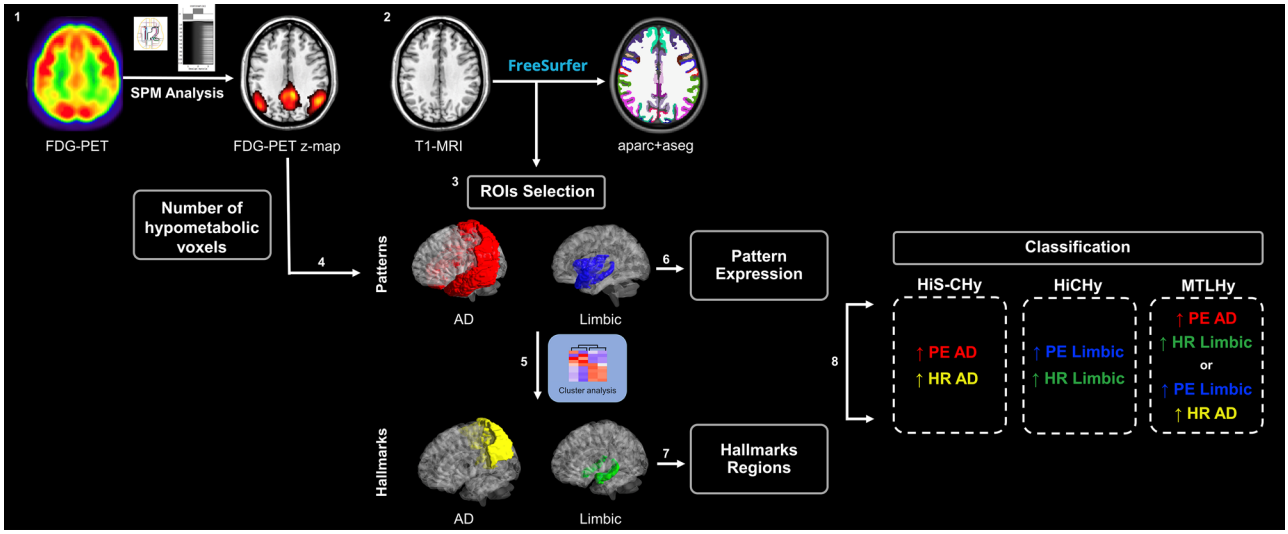

FIGURE 1 Schematic diagram of key steps in the single-subject classification workflow. The steady-state FDG-PET (1) is pre-processed and compared to a healthy controls dataset to obtain a *z*-map of brain hypometabolism. The 3D volumetric MRI (2) is used to generate the FreeSurfer segmentation. AD-like and limbic structures were selected from FreeSurfer labels (3). The number of hypometabolism voxels were extracted from the AD and limbic patterns (4) and a two-step clustering analysis was performed to select the AD and limbic hallmarks (5). The obtained PE (6) and HR (7) were merged to obtain the (8) overall classification. Subjects showing high levels of AD PE and HR were classified as hippocampal-sparing with cortical hypometabolism (HiS-CHy) subtype; subjects with relatively high levels of both AD PE and limbic HR, or limbic PE and AD HR, were classified as Hippocampal and cortical hypometabolism (HiCHy) subtype; subjects with relatively high levels of limbic PE and HR as medial temporal cortex hypometabolism (MTLHy) subtype. AD, Alzheimer's disease; FDG, fluorodeoxyglucose; HR, hallmark region; MRI, magnetic resonance imaging; PE, pattern expression; PET, positron emission tomography; ROI, region of interest; SPM, statistical parametric mapping.

structures, including the hippocampus and its subunits, amygdala, caudate, putamen, ventricles; (5) tessellation of the gray matter–white matter boundary; (6) topology correction; and (7) surface deformation following intensity gradients. Quality control of the processed outputs was performed by experienced neuroscientists who inspected the results slice by slice and discarded those with poor quality or incorrect segmentation.

The typical AD-like temporo-parietal metabolic pattern was constructed by selecting specific FreeSurfer labels. For the temporal lobe, we included superior, middle, and inferior temporal gyri, and superior and middle temporal pole. For the parietal lobe, we included precuneus, angular gyrus and supramarginal gyrus, postcentral gyrus, and paracentral lobule. The posterior cingulum was also included (Figure 1). We selected the brain regions that have been widely described with in vivo imaging in AD patients,[35,36] and in pathologically confirmed AD.[37] These cortical brain structures have shown high burden of AD pathology.[35]

The limbic structures consisted of hippocampus, amygdala, insula, and superior temporal pole (Figure 1). These regions were selected considering previous FDG-PET studies reporting a focal limbic-predominant hypometabolism pattern in aMCI subjects.[26,27] These brain regions have been associated with a high burden of phosphorylated TDP-43, argyrophilic grain accumulation, or hippocampal sclerosis in *post mortem* studies.[25,38]

2.4.2 | FDG-PET pattern expression

The pattern expression (PE) was extracted by considering the SPM *z*-map obtained from SPM single-subject procedure.[31] The PE was defined by counting the statistically significant hypometabolic voxels ($P < 0.05$) within the AD-like and limbic structures for all participants.

$$PE = \frac{number\ of\ hypometabolic\ voxels\ _{(PATTERN)}}{total\ number\ of\ voxels\ _{(PATTERN)}}$$

Each subject was then binary classified according to the highest value between AD or limbic PE (Figure 1).

2.4.3 | Hallmark regions and final classification

We applied a two-step clustering algorithm using the SPM-z scores extracted from the individual AD-like or limbic structures as input (Figure 1). The two-step clustering, by means of a log-likelihood distance criterion, allowed grouping the SPM-z scores into two disjointed clusters. The structures which best represented the two typical AD-like and limbic clusters were then selected by arbitrarily fixing the predictor importance to 0.4. This value allowed us to identify those regions, named the hallmark regions (HR), which produced a noticeable impact in defining the two clusters.[39]

As for the PE, we counted the statistically significant hypometabolic voxels within the obtained pathological HR (Figure 1).

$$HR = \frac{number\ of\ hypometabolic\ voxels\ _{(HALLMARKS)}}{total\ number\ of\ voxels\ _{(HALLMARKS)}}$$

Each subject was binary classified choosing the highest values between typical AD-like or limbic HR. The combination of PE and HR classifications generated three different subtypes expressing specific hypometabolism features (Figure 1).

2.5 | Statistical comparisons

A voxel-wise *t* test on SPM12 procedure was performed between each identified FDG-PET subtype and an internal dataset of 112 HC subjects,[30] considering age as a nuisance variable. The statistical threshold was set at $P = 0.05$, family-wise error (FWE)–corrected for multiple comparisons. Only clusters containing > 100 voxels were deemed significant. This analysis was applied to explore for the presence of laterality, and for hypometabolism voxels outside typical AD-like and limbic structures.

In a post hoc analysis, we evaluated relative hypermetabolism, namely voxels with significantly higher levels of metabolism compared to the HC dataset. This was done to investigate the hypothesis of an increased metabolism at the MTL level in the group that resulted with severe cortical hypometabolism, but hippocampal sparing (see Results section).

A voxel-based morphometry (VBM) on MRI T1, within the SPM12 procedures, was applied to evaluate brain structures in the aMCI subtypes compared to an internal dataset of 382 HC subjects, considering age a nuisance variable. The statistical threshold was set at $P = 0.05$, FWE-corrected for multiple comparisons.

FreeSurfer *z*-scores of volumes and thicknesses were also calculated based on the mean and standard deviation of the 382 HC subjects.

Between-group differences in demographic, clinical, *APOE* ε4 allele (i.e., *APOE* ε3/ε4 or ε4/ε4), CSF, PE and HR, and MRI variables were assessed by applying the analysis of variance test with Bonferroni post hoc correction or the chi-squared test of association when variables were dichotomous. As for CSF and neuropsychological measures, we calculated standardized *z*-scores with a mean of 0 and standard deviation of 1, separately for the two aMCI cohorts. *Z*-scores enabled direct comparison between the two cohorts, avoiding acquisition biases.

CSF *z*-scores were correlated with single-subject PE and HR to evaluate the linear relationship between CSF pathology and the level of brain hypometabolism expression in the three subtypes.

We then applied a voxel-wise linear regression model to assess the contribution of hippocampal atrophy on whole brain metabolism.

2.6 | Follow-up analysis (aMCI-ADNI cohort)

The INTERCEPTOR project is ongoing, and the consortium agreement allows the use of follow-up data only at the project end in December 2023. The follow-up analysis was thus performed only in the aMCI-ADNI cohort, in which MMSE, CDR, FAQ, and IADL scores were available up to the last follow-up (54 ± 22 months), thus providing longitudinal measures of cognitive decline and progression to dementia. MMSE deflection, the number of MMSE points lost per year (annual % rate), was also computed to provide an index of clinical progression.

We applied the Kruskal–Wallis test with Bonferroni post hoc correction and the chi-squared test of association for dichotomous variables, to assess differences across the subtypes stratified according to the clinical progression at follow-up. The clinical progression was defined according to MMSE and CDR changes in the latest follow-up assessment available in the ADNI dataset (i.e., follow-up CDR ≥ 1 and MMSE ≤ 24).

Cox regression analysis was used to assess the ability of the PE and HR measures to predict longitudinal clinical progression over the follow-up time in aMCI subjects. We considered the follow-up time as the time-dependent covariate, and we entered baseline single-subject PE and HR values as possible predictors of clinical conversion at follow-up.

Commonality analysis of whole brain hypometabolism was performed for each subtype stratified by clinical outcomes at follow-up. We used a one-sample *t* test inserting the contrast images resulting from the first level single-subject SPM-based analysis (see the FDG-PET Procedure section) as the dependent variable. The resulting commonalities maps were thresholded at $P < 0.001$, uncorrected for multiple comparisons, with a minimum cluster size of 100 voxels.

Pearson's correlation analysis was applied to evaluate the correlation between FDG-PET PE/HR and CSF *z*-scores in converters and stable aMCI subjects, separately.

Statistical analyses were performed using Statistical Package for the Social Sciences (SPSS v. 27).

3 | RESULTS

3.1 | FDG-PET subtype classification

The two-step clustering analysis identified the superior and inferior parietal lobules and the precuneus, bilaterally, as the AD-like HR, the amygdala and hippocampus, bilaterally, as the limbic HR (Figure 1).

Considering PE and HR classifications, we obtained three aMCI subtypes expressing different hypometabolism features. In detail, $N = 76$ aMCI subjects, classified as hippocampal-sparing with cortical hypometabolism (HiS-CHy), showed significantly higher AD-like PE and HR than typical-AD with hippocampal and cortical hypometabolism (HiCHy; $P < 0.001$) and medial temporal lobe hypometabolism (MTLHy; $P < 0.001$); $N = 34$ classified as HiCHy with significantly higher AD-like PE than MTLHy ($P < 0.001$) and significantly higher limbic HR than HiS-CHy ($P < 0.001$); $N = 97$ classified as MTLHy with significantly higher limbic PE and HR than HiCHy ($P = 0.005$; $P = 0.002$) and HiS-CHy ($P < 0.001$; Table S1 in supporting information).

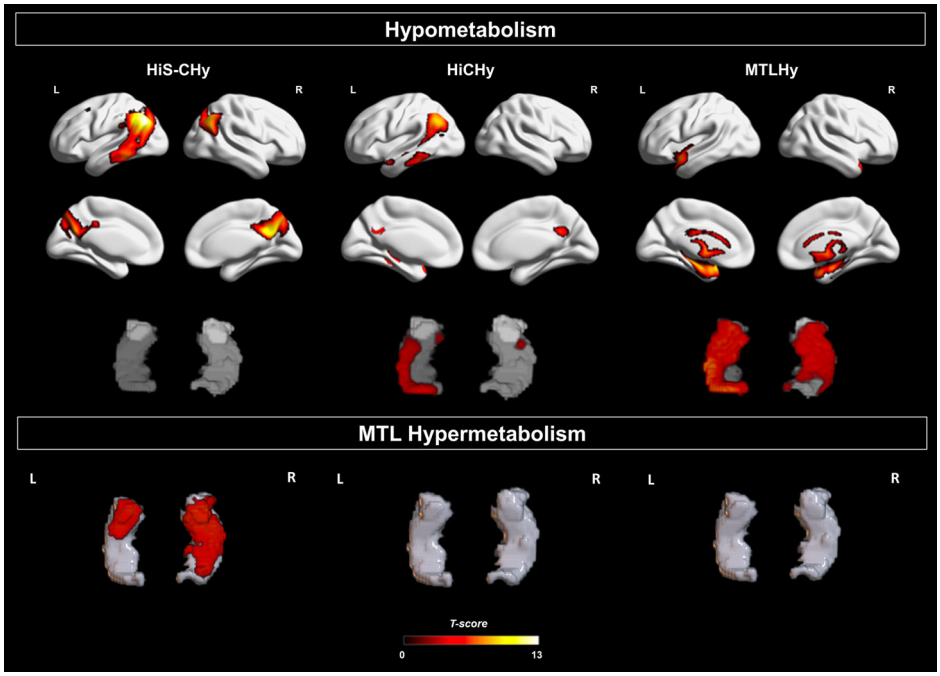

FIGURE 2 Group-analysis. Voxel-wise SPM comparison between aMCI subtypes and FDG-PET database of healthy controls ($N = 112$). Renderings representing significant hypometabolism and hypermetabolism in cortex, amygdala, and hippocampus in HiS-CHy, HiCHy, and MTLHy subtypes. Each comparison was family-wise error–corrected, with a significance level at $P < 0.05$. aMCI, amnestic mild cognitive impairment; FDG, fluorodeoxyglucose; HiS-CHy, hippocampal-sparing with cortical hypometabolism; HiCHy, hippocampal and cortical hypometabolism; MTLHy, medial temporal lobe hypometabolism; PET, positron emission tomography; SPM, statistical parametric mapping.

The HiS-CHy group in the voxel-wise comparison to the HC group showed significant hypometabolism in the angular gyrus, precuneus, middle occipital gyrus, and posterior cingulate cortex, bilaterally, and in the supramarginal gyrus, middle and inferior temporal gyri, on the left. The post hoc analysis showed significant hypermetabolism in hippocampus and amygdala, bilaterally. No other hypermetabolic patterns emerged.

The HiCHy subtype showed a significant hypometabolism prevalent in the left hemisphere, in the angular gyrus, supramarginal gyrus, middle temporal gyrus, superior temporal gyrus, hippocampus and, bilaterally, in the posterior cingulate cortex and precuneus. The HiCHy did not show any significant hypermetabolism at the defined statistical threshold.

The MTLHy subtype showed hypometabolism in the superior temporal gyrus, amygdala, hippocampus, bilaterally, and in the left insula (Figure 2).

The three resulting subtypes did not differ in terms of sex ($P = 0.557$), education ($P = 0.871$) and MMSE score at baseline ($P = 0.370$). Of note, the MTLHy aMCI were significantly older ($P = 0.02$) than the HiS-CHy aMCI subjects.

3.1.1 | CSF features

We found a significantly lower Aβ42 in the HiS-CHy ($P = 0.025$) than in the HiCHy subtype. Further, we found a significantly altered CSF total tau (t-tau; $P = 0.039$) and phosphorylated tau (p-tau)/Aβ42 ratio ($P = 0.004$) in the HiS-CHy subtype than the MTLHy subtype. Also, both HiS-CHy ($P = 0.004$) and HiCHy ($P = 0.025$) showed a higher CSF p-tau/Aβ42 ratio than MTLHy subtype (Table 1).

AD PE ($r = -0.144$, $P = 0.04$) negatively correlated with CSF Aβ42, whereas limbic PE positively correlated with Aβ42 ($r = 0.162$, $P = 0.02$). Thus, a higher expression of the AD-like hypometabolism pattern was associated with a higher level of CSF Aβ42 pathology. Furthermore, both the AD PE and limbic PE correlated with p-tau and the p-tau/Aβ42 ratio levels, but with an opposite slope. Thus, a higher expression of AD-like pattern was associated with more CSF p-tau pathology ($r = 0.143$, $P = 0.04$) and p-tau/Aβ42 ratio ($r = 0.206$, $P = 0.004$) levels, while a higher limbic PE was associated with less pathological levels of p-tau ($r = -0.199$, $P = 0.005$) and p-tau/Aβ42 ratio ($r = -0.176$, $P = 0.01$; Figure 3).

3.1.2 | VBM whole brain

Whole-brain VBM analysis showed no evidence of cortical and subcortical atrophy in the HiS-CHy and HiCHy subtypes compared to the HC group. Only the MTLHy group showed a significant focal atrophy in the left hippocampus.

3.1.3 | Medial temporal thickness

The analysis revealed atrophy of the entorhinal cortices in all groups, with MTLHy showing the greatest extent of shrinkage over two standard deviations.

TABLE 1 Demographic, clinical, genetic, biological, and MRI characteristics of the whole sample (aMCI ADNI-INTERCEPTOR) and across the three subtypes.

	Whole sample	HiS-CHy	HiCHy	MTLHy	*P*-value
N	207	76 [50-26][d]	34 [23-11][d]	97 [53-44][d]	-
Age (years)	73.27 ± 6.3	71.76 ± 6.88	73.44 ± 5.14	74.38 ± 5.94	0.02[a]
Sex (F/M)	107/100	42/34	15/19	50/47	0.557
Education (years)	13.19 ± 4.9	12.96 ± 4.57	13.29 ± 5.88	13.34 ± 4.74	0.871
MMSE (raw score)	26.89 ± 2.05	26.67 ± 1.96	26.79 ± 2.14	27.11 ± 2.07	0.370
RAVLT Del. Recall	[3.96 ± 2.9; 2.65 ± 2.6][d]	0.16 ± 0.73	−0.03 ± 0.99	0.142 ± 1.15	0.129
Semantic Fluency	[17.6 ± 4.05; 26.6 ± 8.6][d]	−0.08 ± 1.03	−0.05 ± 0.98	0.09 ± 0.98	0.501
NPI	[4.8 ± 6.6; 10.9 ± 10.8][d]	0.006 ± 0.95	−0.03 ± 0.99	0.006 ± 1.04	0.980
CDR	0.5	0.5	0.5	0.5	–
FAQ (ADNI)	4.48 ± 5.6	0.05 ± 0.8	0.17 ± 0.99	−0.07 ± 1.1	0.728
IADL (INTERCEPTOR)	9.76 ± 12.1	0.35 ± 1.3	0.02 ± 0.9	−0.27 ± 0.6	0.009[a]
APOE ε4 allele (% Presence)	8.2%	3.9%	17.6%	8.2%	0.04[b]
CSF Aβ1-42	[185.3 ± 142.2; 630.8 ± 346.8 *pg/mL*][d]	−0.24 ± 0.52	0.254 ± 1.5	0.09 ± 1.0	0.025[b]
CSF p-tau	[405.2 ± 268.3; 93.9 ± 55.2][d]	0.19 ± 1.02	0.33 ± 1.1	−0.27 ± 0.85	<0.001[c]
CSF t-tau	[383.1 ± 300.7; 598.1 ± 315.2 *pg/mL*][d]	0.19 ± 1.09	0.08 ± 0.99	−0.18 ± 0.88	0.04[a]
P-tau/Aβ ratio	[2.7 ± 2.1; 0.2 ± 1.2 *pg/mL*][d]	0.22 ± 0.97	0.26 ± 1.14	−0.27 ± 0.89	0.002[c]
T-tau/Aβ ratio	[2.5 ± 2.2; 1.2 ± 0.8 *pg/mL*][d]	0.238 ± 1.45	0.075 ± 0.97	−0.214 ± 0.83	0.012[a]
Left THV MRI	[4003 ± 633; 3982 ± 508 mm^3][d]	−1.16 ± 1.05	−1.22 ± 1.32	−1.53 ± 1.18	0.102
Right THV MRI	[4177 ± 621; 4188 ± 560 mm^3][d]	−1.08 ± 1.13	−1.10 ± 1.55	−1.40 ± 1.19	0.202

Note: Between-group comparisons with significant results at the omnibus test are then post hoc compared applying the Bonferroni correction. *Z* scores were computed for CSF, RAVLT Delayed Recall, Semantic Fluency, NPI, and THV MRI data considering ADNI and INTERCEPTOR cohorts separately.
Abbreviations: Aβ, amyloid beta; ADNI, Alzheimer's Disease Neuroimaging Initiative; aMCI, amnestic mild cognitive impairment; *APOE ε4 allele*, apolipoprotein E ε3/ε4 or ε4/ε4; CDR, Clinical Dementia Rating scale; CSF, cerebrospinal fluid; FAQ, Functional Activities Questionnaire; HiS-CHy, hippocampal-sparing with cortical hypometabolism; HiCHy, hippocampal and cortical hypometabolism; IADL, Instrumental Activities of Daily Living; MTLHy, medial temporal lobe hypometabolism; MMSE, Mini-Mental State Examination; MRI, magnetic resonance imaging; NPI, Neuropsychiatric Inventory; p-tau, phosphorylated tau; RAVLT Del. Recall, Rey Auditory Verbal Learning Test Delayed Recall; THV, total hippocampal volume; t-tau, total tau.
[a]HiS-CHy ≠ MTLHy.
[b]HiCHy ≠ HiS-CHy.
[c]MTLHy ≠ HiCHy and HiS-CHy.
[d][aMCI ADNI-INTERCEPTOR].

3.1.4 | Comparison of FDG-PET hypometabolism and hippocampal atrophy

The voxel-wise regression analysis showed that the hippocampal atrophy significantly contributed to a more severe hypometabolism in left PCC (t = 6.74; MNI coordinates = −4, −30, 32; $P < 0.001$), left hippocampus (t = 7.36; MNI coordinates = −28, 12, −26; $P < 0.001$), and right middle cingulate cortex (t = 6.54; MNI coordinates = 6, −22, 32; $P < 0.001$).

3.1.5 | Follow-up analysis (aMCI-ADNI cohort)

At the latest follow-up time available (≈5-year) in the aMCI-ADNI cohort, the HiS-CHy subtype showed the highest conversion rate to dementia due to AD (73%). The MTLHy showed a conversion rate to dementia of 34%, significantly lower than the other two subtypes (P = 0.006); most of them remaining clinically stable over long time. Of note, these data indicate a continuum within the cohorts with the HiS-CHy converters and the MTLHy stable subtypes at the extremes. Also, clinical data in terms of CDR, MMSE deflection, and CSF biomarkers reflect the large gap between the HiS-CHy converters and stable MTLHy subtype (Table 2).

The presence of an AD-like hypometabolism (high AD-like PE) was significantly associated with the greatest conversion to dementia with a hazard risk ratio of 78.52 (95% confidence interval [CI]: 5.9–1047.4). The limbic PE was inserted in the Cox regression model with a hazard risk ratio of 0.07 (95% CI: 0.01–0.47), but with an opposite β coefficient (β = −2.62, P = 0.006) compared to the AD-like PE (β = 4.363, P = 0.001), meaning that a higher level of limbic PE was less associated with progression to dementia.

In each subtype, converters always showed presence of cortical hypometabolism at difference with the stable aMCI (Figure 4A).

In all the aMCI converters, the correlation analysis of CSF measures and brain hypometabolism at baseline was significant for p-tau/Aβ42 ratio and AD-like HR (Figure 4B). This means that a more significant and

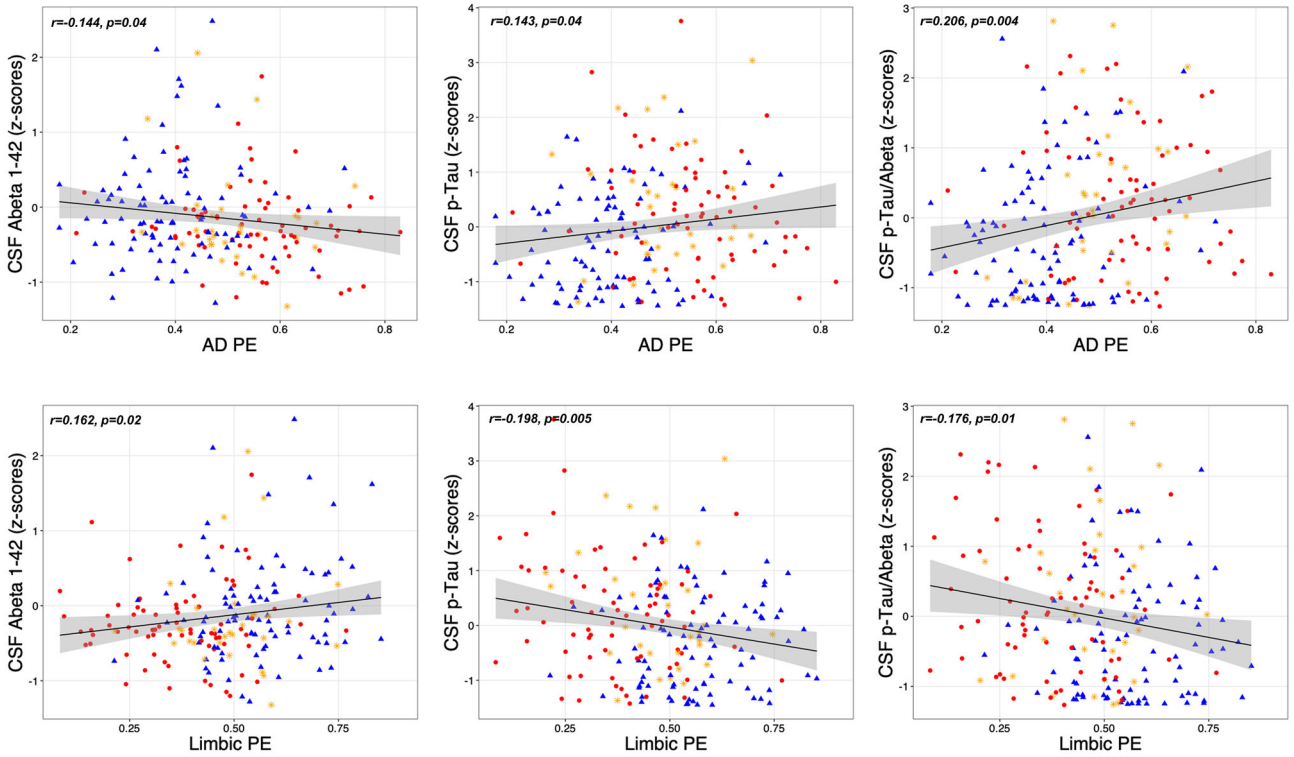

FIGURE 3 AD-like/limbic PE and CSF-AD biomarkers relationship. Scatterplots show linear association between PE and CSF-AD biomarkers in the whole sample. Red circles represent the HiS-CHy, yellow asterisks represent the HiCHy, and blue triangles represent the MTLHy subtype. AD, Alzheimer's disease; CSF, cerebrospinal fluid; HiS-CHy, hippocampal-sparing with cortical hypometabolism; HiCHy, hippocampal and cortical hypometabolism; MTLHy, medial temporal lobe hypometabolism; PE, pattern expression; p-tau, phosphorylated tau.

extended hypometabolism in AD-like hallmark regions was associated with a more pathological level of p-tau/Aβ42 ratio ($r = 0.395$, $P = 0.01$). On the contrary, the limbic HR was associated with less pathological levels of p-tau/Aβ42 ratio ($r = -0.422$, $P = 0.007$).

4 | DISCUSSION

The use of multiple biomarkers in the prodromal stage is crucial to identify those MCI subjects—expecting to convert to AD dementia with 10% to 15% annual rate—when functional disability is still absent.[40]

The co-occurrence of multiple biomarker alterations is associated with a steeper cognitive decline and a higher risk of dementia.[1,19,41] In the amyloid/tau/neurodegeneration classification system, the amyloid and tau pathology supports the diagnosis of AD as a biological entity.[5] However, the pure biological definition of AD entails some limitations: Aβ does not help to differentiate among AD clinical phenotypes, because cortical Aβ deposition is widely distributed across the entire cortex without specific topography.[42] Amyloid-PET positivity is reported in non-AD conditions[43,44] and in normal aging adults.[45] The co-occurrence of Aβ and tau pathology, both in normal individuals and in MCI, does not always predate AD dementia[46] and amyloidopathy is insufficient to define AD without clinical correspondence.[47]

A spatio-temporal relationship between pathology and neurodegeneration was reported throughout the AD continuum.[7] Growing evidence suggests that Aβ and tau pathologies act in concert in synapse degeneration[48] and as triggers of downstream pathways, including facilitation of tau spreading and tau-mediated neurotoxicity.[49] In vivo evidence has shown that tau pathology significantly covaries with FDG-PET brain hypometabolism in most brain regions, irrespective of Aβ.[14,50]

Regional patterns of decreased FDG-PET is the result of both local pathology and long-distance processes of deafferentation,[7,51] capturing changes beyond MRI atrophy.[52] Moreover, neurodegeneration, as measured by FDG-PET, strongly correlates with cognitive decline and is detectable even before clinical symptom onset.[53,54] Thus, FDG-PET has been recognized as one of the most accurate biomarkers in predicting the possible progression from MCI to dementia, but also in recognizing those subjects remaining clinically stable over time.[19,26,27]

Here, we used FDG-PET brain metabolism as biomarker of neurodegeneration and investigated the relationship with AD biological profiles. We distinguished three aMCI subtypes, based on FDG-PET hypometabolism features, with a comparable neuropsychological phenotype at baseline and different risk of progression. We suggest that these specific patterns of brain hypometabolism, irrespective to the MRI and CSF Aβ and tau status, were able to identify subtypes representative of diverse biological entities.

The HiS-CHy subtype with high positivity of AD-CSF biomarkers and the highest level of cognitive decline and progression to AD dementia (73%), represents the most malignant phenotype. This

TABLE 2 Demographic, clinical, and biomarkers features across the stable (S) and converters (C) aMCI-ADNI subtypes.

	HiS-CHy (S)	HiS-CHy (C)	HiCHy (S)	HiCHy (C)	MTLHy (S)	MTLHy (C)	*p*-value
%	27%	73%	45%	55%	66%	34%	-
Age at follow-up (years)	66.7 ± 6.9	70.8 ± 6.9	74.2 ± 6.3	70.0 ± 3.5	74.3 ± 7.1	74.1 ± 5.4	**0.009**[d]
Follow-up time (months)	51.5 ± 15.3	44.3 ± 14.5	38.4 ± 15.6	45.7 ± 10.7	64.3 ± 26.6	54.1 ± 20.8	**0.02**[a]
Sex (F/M)	2/5	11/8	2/3	3/3	13/16	4/11	0.532
Education (years)	16.6 ± 1.8	16.6 ± 2.0	16.6 ± 2.6	16.5 ± 2.9	16.4 ± 2.9	15.9 ± 2.6	0.953
RAVLT Del. Recall	−0.01 ± 0.4	−0.4 ± 0.3	0.1 ± 0.9	−0.4 ± 0.1	0.2 ± 0.1	0.1 ± 1.9	0.289
Semantic Fluency	0.5 ± 0.8	−0.7 ± 0.8	0.4 ± 0.9	−0.5 ± 1.2	0.6 ± 0.7	−0.6 ± 0.7	<**0.001**[a,b]
NPI	−0.5 ± 0.6	0.2 ± 1.2	−0.2 ± 0.7	1.1 ± 1.6	−0.5 ± 0.4	0.6 ± 0.9	<**0.001**[b,e]
MMSE raw score (baseline)	28.3 ± 1.9	27.4 ± 1.6	27.4 ± 1.1	27.5 ± 1.4	27.4 ± 1.6	28.2 ± 1.4	**0.007**[b]
MMSE raw score (follow-up)	27.0 ± 2.1	23.7 ± 3.5	26.6 ± 2.6	24.8 ± 1.9	27.53 ± 1.8	21.8 ± 1.6	<**0.001**[b,c,d]
MMSE deflection (annual % Rate)	−2.8%	−8.8%	−2.9%	−5.8%	−1.4%	−9.0%	<**0.001**[a]
CDR (baseline)	0.5	0.5	0.5	0.5	0.5	0.5	–
CDR (follow-up)	0.57 ± 0.2	1.1 ± 0.4	0.5 ± 1.1	1.1 ± 1.3	0.5 ± 0.6	1.4 ± 1.2	**0.012**[a]
Left THV MRI (z-score)	−1.63 ± 1.32	−1.22 ± 1.03	−0.31 ± 2.48	−1.47 ± 0.97	−1.19 ± 1.40	−1.80 ± 1.05	0.578
Right THV MRI (z-score)	−1.68 ± 0.93	−1.07 ± 1.11	0.53 ± 2.30	−1.86 ± 0.80	−1.17 ± 1.28	−1.77 ± 1.11	0.071
APOE ε4 allele (% Presence)	57.1%	63.2%	60%	66.7%	34.5%	66.7%	0.260
CSF Aβ1-42 (% Pathol.)	85.7%	100%	100%	67%	48.3%	80%	**0.002**[a,f]
CSF p-tau (% pathol.)	100%	100%	100%	100%	86%	100%	0.183
CSF t-tau (% pathol.)	100%	100%	80%	83.3%	82.8%	93.3%	0.339

Notes: Between-group comparisons resulting significant at the omnibus test are then post hoc compared applying the Bonferroni correction. *Z* scores were computed for RAVLT Delayed Recall, Semantic Fluency, NPI, and THV MRI data. CSF Aβ1-42 cut-off < 192 pg/mL; CSF p-tau cut-off > 23 pg/mL; CSF t-tau cut-off > 93 pg/mL.

Abbreviations: Aβ, amyloid beta; ADNI, Alzheimer's Disease Neuroimaging Initiative; aMCI, amnestic mild cognitive impairment; *APOE ε4 allele*, apolipoprotein E ε3/ε4 or ε4/ε4 genotype; CDR, Clinical Dementia Rating scale; CSF, cerebrospinal fluid; FAQ, Functional Activities Questionnaire; HiS-CHy, hippocampal-sparing with cortical hypometabolism; HiCHy, hippocampal and cortical hypometabolism; IADL, Instrumental Activities of Daily Living; MTLHy, medial temporal lobe hypometabolism; MMSE, Mini-Mental State Examination; MRI, magnetic resonance imaging; NPI, Neuropsychiatric Inventory; p-tau, phosphorylated tau; RAVLT Del. Recall, Rey Auditory Verbal Learning Test Delayed Recall; THV, total hippocampal volume; t-tau, total tau.

[a]HiS-CHy (C) ≠ MTLHy (S).
[b]MTLHy (C) ≠ MTLHy (S).
[c]HiS-CHy (C) ≠ HiS-CHy (S).
[d]MTLHy (C) ≠ HiS-CHy (S).
[e]HiS-CHy (S) ≠ HiCHy (C).
[f]HiCHy (S) ≠ MTLHy (S).

finding is consistent with previous studies that identified patients with fast progression and younger age at death, presenting with a diffuse atrophy and tau pathology in associative cortices as the most aggressive form of AD.[9,55,56] Consistently, here, a high expression of hypometabolism in the AD HR, but hippocampal sparing, was significantly associated with p-tau/Aβ ratio pathology and conversion to dementia. A crucial finding is the lack of hypometabolism in the MTL in this subtype. A possible factor may be a reduced tau burden in MTL structures, in contrast to a severe tau load in the associative cortices, which has been reported by both *post mortem*[56] and PET neuroimaging.[14,55] We further explored this issue by investigating the presence of relative MTL hypermetabolism. Only the HiS-CHy group showed a relative increase of metabolism in MTL structures compared to HC. Glucose hypermetabolism of hippocampus and amygdala has been reported in aMCI[57] and subjective cognitive decline,[54] and was suggested as an early downstream consequence to neuropathology, or an attempt of the affected brain regions to promote resilience.[54,57] Of note, the hippocampal hyperactivity has been associated with a detrimental response contributing to memory impairment in aMCI.[58] All the above suggested mechanisms could explain the co-presence, of diffuse cortical hypometabolism and MTL hypermetabolism in the HiS-CHy subtype.

The HiCHy group showed cortical hypometabolism concomitant with MTL hypometabolism. A longitudinal clinico-pathological study found that typical AD-like hypometabolism can progress from the hippocampus to the temporo-parietal and posterior cingulate cortices at the MCI stage, with a variably lateralized pattern.[51] The hippocampal dysfunction and atrophy may trigger cortical degeneration through the cingulate bundle[59] and fornix[60] tracts, interconnecting these structures. Consistently, we found that reduced hippocampal thickness was

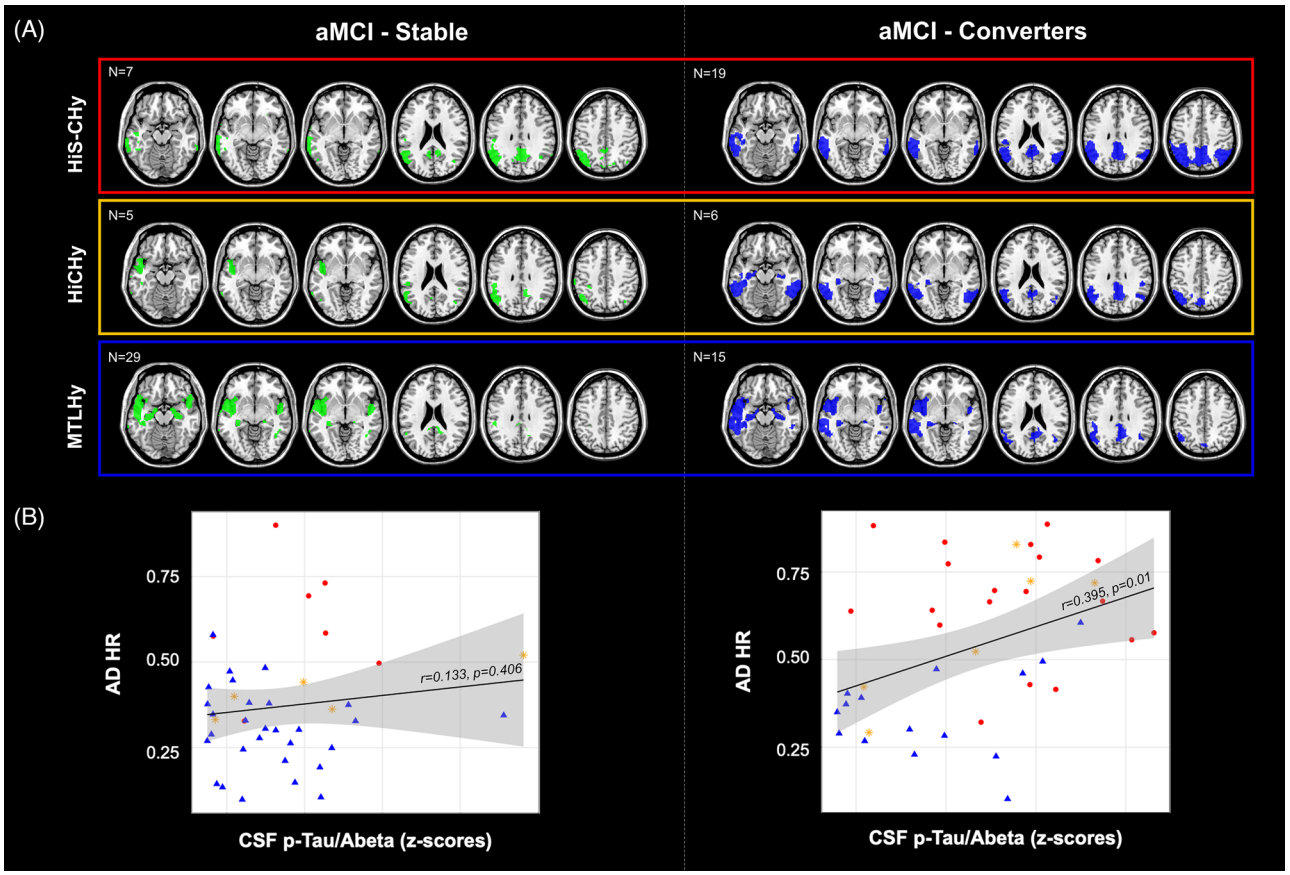

FIGURE 4 Brain hypometabolism differences between stable and converter aMCI subjects. A, The FDG-PET hypometabolism patterns overlaid on a T1-MRI template image in the three aMCI-ADNI subtypes according to the clinical progression at follow-up. B, Scatterplots showing Pearson's correlation between the levels of hypometabolism expression in AD HR and p-tau/Aβ42 ratio significant at $P < 0.05$. Aβ, amyloid beta; AD, Alzheimer's disease; ADNI, Alzheimer's Disease Neuroimaging Initiative; aMCI, amnestic mild cognitive impairment; CSF, cerebrospinal fluid; HiS-CHy, hippocampal-sparing with cortical hypometabolism (converters = 19, stable = 7); HiCHy, hippocampal and cortical hypometabolism (converters = 6, stable = 5); HR, hallmark regions; MTLHy, medial temporal lobe hypometabolism (converters = 15, stable = 29); p-tau, phosphorylated tau.

significantly associated with decreased FDG-PET signal in the PCC. Moreover, a decreased functional connectivity between hippocampus and PCC was found to co-localize with regions of highest tau and Aβ deposition.[61] Of note, the HiCHy subtype also showed the highest proportion of *APOE* ε4 allele carriers, and the *APOE* ε4 allele was associated with the severity of MTL hypometabolism.[62] This is consistent also with evidence that *APOE* ε4 allele is associated with an amnestic phenotype and more severe hippocampal atrophy.[63] The HiCHy, as well the HiS-CHy subtype, had the highest CSF p-tau and p-tau/Aβ ratio.

In contrast, the MTLHy showed the lowest conversion rate (34%) and limited amount of CSF-AD pathology. The pure amnestic syndrome, associated with old age, and a slow or absent cognitive decline, represents the clinical signatures of this condition, together with heterogeneous CSF biomarker abnormalities.[26,27] The clinically benign course over long follow-up periods has suggested the presence of different pathological substrates. Hippocampal sclerosis was suggested as the main cause of memory loss in stable aMCI.[64] Other possible etiologies include primary age-related tauopathy, which lacks of pathological amyloid load,[65] and limbic-predominant age-related TDP-43 encephalopathy, a TDP-43 proteinopathy with or without concomitant amyloidopathy.[25] Previous studies by our group reported a consistent rate of clinically stable aMCI, from 16% to 38% of the cohorts, showing a selective MTL hypometabolism.[26,27] This condition cannot be attributed only to the AD spectrum, as recently reported,[55] but also to non-AD pathology with possibly more benign course.[25,66] This FDG-PET evidence in aMCI has undeniable prognostic and therapeutic repercussions, also for the design of pharmacological clinical trials of disease-modifying drugs, excluding no-AD individuals who will never develop AD dementia.

In our continuum model, the selective posterior vulnerability is associated with increased AD-related CSF changes and higher risk of conversion to dementia. In a gray area there was a percentage of HiS-CHy (27%) and HiCHy (45%) with no progression to dementia in the considered follow-up time. This indicates a possible wide time range for clinical progression in aMCI even in cases with multiple specific biomarker positivity.[67] Other factors such as brain resilience, cognitive-brain reserve, and compensation should be considered,[68] and longer longitudinal studies are necessary. The algorithm also

classified as MTLHy a percentage of subjects who progressed to dementia, showing at individual level not only a severe MTL hypometabolism, but also a limited, initial hypometabolism in the posterior cortex. The additional presence of *APOE* ε4 allele in most of them leads us to consider those aMCI as a predominant limbic AD type.[62]

The HiS-CHy and HiCHy subtypes shared the presence of an asymmetry of the hypometabolism pattern prevalent on the left. A left-lateralized hypometabolism pattern was reported in early stages of AD; it parallels distributions of NFT[69] and Aβ plaques,[70] and becomes more symmetrical as disease progresses.[71,72]

VBM MRI assessment revealed no significant cortical atrophy in each subtype in the comparison to the reference control group, also at individual level. Our findings in prodromal aMCI phase support previous evidence in AD and other neurodegenerative diseases, that synaptic dysfunction—as detected by FDG-PET—and neuronal death—as measured by structural MRI—are measures of neurodegeneration that occur at different times. Thus, the two measures should not be considered interchangeable measures of neurodegeneration.[14] On the other hand, the evaluation of hippocampal volume and thickness showed that atrophy was present, but more pronounced in MTLHy than in the other two subtypes, even though without statistical significance.

With an abundance of big data available, novel computational approaches using AI represent an emerging field of interest. AI was applied to FDG-PET data for the early diagnosis of AD, providing 86.4% accuracy in identifying MCI individuals who will convert to AD dementia within 1 to 3 years.[73] Another study aimed to use AI to develop an age prediction model based on structural MRI and FDG-PET in normal and neurodegenerative conditions.[17] FDG-based brain age prediction showed a better performance than MRI in predicting chronological age, supporting the role of FDG-PET hypometabolism as a more sensitive measure of aging trajectories.[17] The main challenge for the application of AI in the clinical routine is the overfitting that arises when a model is too dependent on a training dataset and is not able to provide good classifications in new clinical data.[74] Furthermore, the population heterogeneity could affect the training dataset and thus the performance of the algorithms.[74] Our results, disentangling aMCI heterogeneity and providing hypometabolic hallmarks, at single subject level, for each identified subtype, might serve for future diagnostic procedures, for example, innovative computational pipelines.

5 | CONCLUSIONS

This study reports the early metabolic changes in subjects with comparable amnestic-type MCI. The obtained results can guide the use of FDG-PET brain hypometabolism as a diagnostic biomarker for aMCI in clinical routine. The presence of FDG-PET hypometabolism in AD-like HR, that is, superior, and inferior parietal lobule and precuneus, confirms a more certain clinical diagnosis of AD, as it demonstrated a relevant relationship with CSF measures and steeper progression to dementia. Of note, MTL hypometabolism defines a clinically benign course and non-AD condition, possibly not on a trajectory to dementia. Our findings support the urgent need to capture heterogeneity at the different levels of neurodegeneration expression and risk of progression, in the early cognitive decline.

AUTHOR CONTRIBUTIONS

Silvia Paola Caminiti, Alberto Redolfi, Daniela Perani contributed to conception and design of the study. Silvia Paola Caminiti, Silvia De Francesco, and Alice Galli contributed to the analysis of data or preparing the figures. Daniela Perani and Alberto Redolfi contributed to the acquisition of data. Silvia Paola Caminiti, Silvia De Francesco, Giacomo Tondo, Alice Galli, Alberto Redolfi, and Daniela Perani contributed to drafting and revision of the text.

ACKNOWLEDGMENTS

The authors are grateful to the Italian Ministry of Health and to the Italian Medicines Agency for their full sponsorship and technical support of the INTERCEPTOR Project. The significant contribution of the following researchers and clinicians is also acknowledged: Maurizio Belfiglio, Francesca Miraglia, Cristina Muscio, Emanuele Cassetta (AFAR, Roma), Mario Barbagallo (ALMA, Palermo), Carlo Gabelli (AOP Padova), Simona Luzzi (AOU, Ancona), Fulvio Lauretani (AOU, Parma), Innocenzo Rainero (AOU, Torino), Carlo Ferrarese (ASST, Monza), Orazio Zanetti (FBF, Brescia), Michela Marcon (Ospedale San Bortolo, Vicenza), Flavio Nobili Mariano (HSANMartino, Genova), Giuseppe Pelliccioni (INRCA, Ancona), Sabina Capellari (ISNB, Bologna), Elena Sinforiani (IRCSS Mondino, Pavia), Gioacchino Tedeschi (Policlinico, Napoli), Carmen Gerace (San Camillo Forlanini, Roma), Laura Bonanni (UNICH, Chieti), Sandro Sorbi (AOU-Careggi, Firenze), Lucilla Parnetti (UniPG, Perugia). Data collection and sharing for this project were funded by the ADNI (National Institutes of Health Grant U01 AG024904) and DOD ADNI (Department of Defense award number W81XWH12-2-0012). ADNI is funded by the National Institute on Aging, the National Institute of Biomedical Imaging and Bioengineering, and through generous contributions from the following groups: AbbVie; Alzheimer's Association; Alzheimer's Drug Discovery Foundation; Araclon Biotech; BioClinica, Inc.; Biogen; Bristol-Myers Squibb Company; CereSpir, Inc.; Cogstate; Eisai Inc.; Elan Pharmaceuticals, Inc.; Eli Lilly and Company; EuroImmun; F. Hoffmann-La Roche Ltd and its affiliated company Genentech, Inc.; Fujirebio; GE Healthcare; IXICO Ltd.; Janssen Alzheimer Immunotherapy Research & Development, LLC; Johnson & Johnson Pharmaceutical Research & Development LLC; Lumosity; Lundbeck; Merck & Co., Inc.; Meso Scale Diagnostics, LLC; NeuroRx Research; Neurotrack Technologies; Novartis Pharmaceuticals Corporation; Pfizer Inc.; Piramal Imaging; Servier; Takeda Pharmaceutical Company; and Transition Therapeutics. The Canadian Institutes of Health Research provided funding to support the ADNI clinical sites in Canada. Private sector contributions are facilitated by the Foundation for the National Institutes of Health (http://www.fnih.org/). The grantee organization is the Northern California Institute for Research and Education, and the study is coordinated by the Alzheimer's Therapeutic Research Institute at the University of Southern California. ADNI data are disseminated

by the Laboratory for Neuro Imaging at the University of Southern California.

Open access funding provided by BIBLIOSAN.

CONFLICTS OF INTEREST STATEMENT

The authors declare no conflicts of interest. Author disclosures are available in the supporting information.

CONSENT STATEMENT

Written informed consent was obtained from participants. Data was used in the current study and the study was approved by all relevant ethic boards related to ADNI and Interceptor projects. The study was conducted in compliance with the Declaration of Helsinki for the protection of human participants.

ORCID

Silvia Paola Caminiti https://orcid.org/0000-0003-4568-1738

REFERENCES

1. Dubois B, Feldman HH, Jacova C, et al. Advancing research diagnostic criteria for Alzheimer's disease: the IWG-2 criteria. *Lancet Neurol* 2014;13:614-629.
2. Aisen PS, Andrieu S, Sampaio C, et al. Report of the task force on designing clinical trials in early (predementia) AD. *Neurology* 2011;76:280-286.
3. Nettiksimmons J, DeCarli C, Landau S, Beckett L, Initiative ADN. Biological heterogeneity in ADNI amnestic mild cognitive impairment. *Alzheimers Dement* 2014;10:511-521.
4. Marra C, Villa G, Quaranta D, Valenza A, Vita MG, Gainotti G. Probable Alzheimer's disease patients presenting as focal temporal lobe dysfunction show a slow rate of cognitive decline. *J Int Neuropsychol Soc* 2012;18:144-150. doi:10.1017/S1355617711001287
5. Jack CR, Bennett DA, Blennow K, et al. NIA-AA research framework: toward a biological definition of Alzheimer's disease. *Alzheimers Dement* 2018;14:535-562. doi:10.1016/j.jalz.2018.02.018
6. Kovacs GG, Milenkovic I, Wöhrer A, et al. Non-Alzheimer neurodegenerative pathologies and their combinations are more frequent than commonly believed in the elderly brain: a community-based autopsy series. *Acta Neuropathol* 2013;126:365-384.
7. Chételat G, Arbizu J, Barthel H, et al. Amyloid-PET and 18F-FDG-PET in the diagnostic investigation of Alzheimer's disease and other dementias. *Lancet Neurol* 2020;19:951-962.
8. Perani D, Iaccarino L, Lammertsma AA, et al. A new perspective for advanced positron emission tomography–based molecular imaging in neurodegenerative proteinopathies. *Alzheimers Dement* 2019;15:1081-1103.
9. Ferreira D, Nordberg A, Westman E. Biological subtypes of Alzheimer disease: a systematic review and meta-analysis. *Neurology* 2020;94:436-448. doi:10.1212/WNL.0000000000009058
10. Ossenkoppele R, van der Kant R, Hansson O. Tau biomarkers in Alzheimer's disease: towards implementation in clinical practice and trials. *Lancet Neurol* 2022. 21.8:726-734.
11. van Eimeren T, Bischof GN, Drzezga A. Is tau imaging more than just upside-down 18F-FDG imaging? *J Nucl Med* 2017;58:1357-1359.
12. Nelson PT, Alafuzoff I, Bigio EH, et al. Correlation of Alzheimer disease neuropathologic changes with cognitive status: a review of the literature. *J Neuropathol Exp Neurol* 2012;71:362-381.
13. Stoessl AJ. Glucose utilization: still in the synapse. *Nat Neurosci* 2017;20:382-384.
14. Strom A, Iaccarino L, Edwards L, et al. Cortical hypometabolism reflects local atrophy and tau pathology in symptomatic Alzheimer's disease. *Brain* 2022;145:713-728.
15. Shaffer JL, Petrella JR, Sheldon FC, et al. Predicting cognitive decline in subjects at risk for Alzheimer disease by using combined cerebrospinal fluid, MR imaging, and PET biomarkers. *Radiology* 2013;266:583-591.
16. Perani D, Caminiti SP, Carli G, Tondo G. PET neuroimaging in dementia conditions. *PET and SPECT in Neurology* 2021:211-282.
17. Lee J, Burkett BJ, Min H-K, et al. Deep learning-based brain age prediction in normal aging and dementia. *Nat Aging* 2022;2:412-424.
18. Perani D. FDG-PET and amyloid-PET imaging: the diverging paths. *Curr Opin Neurol* 2014;27:405-413.
19. Caminiti SP, Ballarini T, Sala A, et al. FDG-PET and CSF biomarker accuracy in prediction of conversion to different dementias in a large multicentre MCI cohort. *Neuroimage Clin* 2018;18:167-177. doi:10.1016/j.nicl.2018.01.019
20. Chetelat G, Desgranges B, De La Sayette V, Viader F, Eustache F, Baron J-C. Mild cognitive impairment: can FDG-PET predict who is to rapidly convert to Alzheimer's disease? *Neurology* 2003;60:1374-1377.
21. Sörensen A, Blazhenets G, Rücker G, et al. Prognosis of conversion of mild cognitive impairment to Alzheimer's dementia by voxel-wise Cox regression based on FDG PET data. *Neuroimage Clin* 2019;21:101637.
22. Protas HD, Chen K, Langbaum JBS, et al. Posterior cingulate glucose metabolism, hippocampal glucose metabolism, and hippocampal volume in cognitively normal, late-middle-aged persons at 3 levels of genetic risk for Alzheimer disease. *JAMA Neurol* 2013;70:320-325.
23. Nestor PJ, Fryer TD, Smielewski P, Hodges JR. Limbic hypometabolism in Alzheimer's disease and mild cognitive impairment. *Ann Neurol* 2003;54:343-351.
24. Mosconi L, Tsui W-H, De Santi S, et al. Reduced hippocampal metabolism in MCI and AD: automated FDG-PET image analysis. *Neurology* 2005;64:1860-1867.
25. Nelson PT, Dickson DW, Trojanowski JQ, et al. Limbic-predominant age-related TDP-43 encephalopathy (LATE): consensus working group report. *Brain* 2019;142:1503-1527. doi:10.1093/brain/awz099
26. Tondo G, Carli G, Santangelo R, et al. Biomarker-based stability in limbic-predominant amnestic mild cognitive impairment. *Eur J Neurol* 2021;28:1123-1133. doi:10.1111/ene.14639
27. Cerami C, Dodich A, Iannaccone S, et al. A biomarker study in long-lasting amnestic mild cognitive impairment. *Alzheimers Res Ther* 2019;10. doi:10.1186/s13195-018-0369-8
28. Rossini PM, Cappa SF, Lattanzio F, et al. The Italian INTERCEPTOR project: from the early identification of patients eligible for prescription of antidementia drugs to a nationwide organizational model for early Alzheimer's disease diagnosis. *J Alzheimers Dis* 2019;72:373-388. doi:10.3233/JAD-190670
29. Petersen RC. Mild cognitive impairment as a diagnostic entity. *J Intern Med* 2004;256:183-194.
30. Perani D, Della Rosa PA, Cerami C, et al. Validation of an optimized SPM procedure for FDG-PET in dementia diagnosis in a clinical setting. *Neuroimage Clin* 2014;6:445-454. doi:10.1016/j.nicl.2014.10.009
31. Della Rosa PA, Cerami C, Gallivanone F, et al. A standardized [18F]-FDG-PET template for spatial normalization in statistical parametric mapping of dementia. *Neuroinformatics* 2014;12:575-593.
32. Caminiti SP, Sala A, Presotto L, et al. Validation of FDG-PET datasets of normal controls for the extraction of SPM-based brain metabolism maps. *Eur J Nucl Med Mol Imaging* 2021;48:2486-2499.
33. Tustison NJ. "N4ITK: improved N3 bias correction,." *IEEE TMI* 2010;29:1310-1320.
34. De Francesco S, Galluzzi S, Vanacore N, et al. Norms for automatic estimation of hippocampal atrophy and a step forward for applicability to the Italian population. *Front Neurosci* 2021; 15: 656808.
35. Jagust W. Imaging the evolution and pathophysiology of Alzheimer disease. *Nat Rev Neurosci* 2018;19:687-700.

36. McKhann GM, Knopman DS, Chertkow H, et al. The diagnosis of dementia due to Alzheimer's disease: recommendations from the National Institute on Aging-Alzheimer's Association workgroups on diagnostic guidelines for Alzheimer's disease. *Alzheimers Dement* 2011;7:263-269.
37. Hoffman JM, Welsh-Bohmer KA, Hanson M, et al. FDG PET imaging in patients with pathologically verified dementia. *J Nucl Med* 2000;41:1920-1928.
38. Bell WR, An Y, Kageyama Y, et al. Neuropathologic, genetic, and longitudinal cognitive profiles in primary age-related tauopathy (PART) and Alzheimer's disease. *Alzheimers Dement* 2019;15:8-16.
39. Köhn H, Hubert LJ. Hierarchical cluster analysis. *Wiley StatsRef: Statistics Reference Online* 2014:1-13.
40. Frisoni GB, Boccardi M, Barkhof F, et al. Strategic roadmap for an early diagnosis of Alzheimer's disease based on biomarkers. *Lancet Neurol* 2017;16:661-676.
41. Cerami C, della Rosa PA, Magnani G, et al. Brain metabolic maps in Mild Cognitive Impairment predict heterogeneity of progression to dementia. *Neuroimage Clin* 2015;7:187-194.
42. Rabinovici GD, Carrillo MC, Forman M, et al. Multiple comorbid neuropathologies in the setting of Alzheimer's disease neuropathology and implications for drug development. *Alzheimers Dement* 2017;3:83-91.
43. Donaghy PC, Firbank MJ, Thomas AJ, et al. Clinical and imaging correlates of amyloid deposition in dementia with Lewy bodies. *Mov Disord* 2018;33:1130-1138.
44. Ossenkoppele R, Jansen WJ, Rabinovici GD, et al. Prevalence of amyloid PET positivity in dementia syndromes: a meta-analysis. *JAMA* 2015;313:1939-1950.
45. La Joie R, Perrotin A, de La Sayette V, et al. Hippocampal subfield volumetry in mild cognitive impairment, Alzheimer's disease and semantic dementia. *Neuroimage Clin* 2013;3:155-162.
46. Hanseeuw BJ, Betensky RA, Jacobs HIL, et al. Association of amyloid and tau with cognition in preclinical Alzheimer disease: a longitudinal study. *JAMA Neurol* 2019;76:915-924.
47. Dubois B, Villain N, Frisoni GB, et al. Clinical diagnosis of Alzheimer's disease: recommendations of the International Working Group. *Lancet Neurol* 2021;20:484-496.
48. Ittner LM, Götz J. Amyloid-β and tau—a toxic pas de deux in Alzheimer's disease. *Nat Rev Neurosci* 2011;12:67-72.
49. Hampel H, Hardy J, Blennow K, et al. The amyloid-β pathway in Alzheimer's disease. *Mol Psychiatry* 2021;26:5481-5503.
50. Bischof GN, Jessen F, Fliessbach K, et al. Impact of tau and amyloid burden on glucose metabolism in Alzheimer's disease. *Ann Clin Transl Neurol* 2016;3:934-939.
51. Mosconi L, Mistur R, Switalski R, et al. FDG-PET changes in brain glucose metabolism from normal cognition to pathologically verified Alzheimer's disease. *Eur J Nucl Med Mol Imaging* 2009;36:811-822.
52. Shaffer JL, Petrella JR, Sheldon FC, et al. Predicting cognitive decline in subjects at risk for Alzheimer disease by using combined cerebrospinal fluid, MR imaging, and PET biomarkers. *Radiology* 2013;266:583.
53. Tondo G, Boccalini C, Vanoli EG, et al. Brain metabolism and amyloid load in individuals with subjective cognitive decline or pre–mild cognitive impairment. *Neurology* 2022; 99.3: e258-e269.
54. Yu X, Zhu Z, Zheng S, Jiang J, Jiang J, Chu Z. In vivo assessment of amyloid and glucose signatures in subjective cognitive decline subjects. *J Mech Med Biol* 2021;21:2140018.
55. Ossenkoppele R, Lyoo CH, Sudre CH, et al. Distinct tau PET patterns in atrophy-defined subtypes of Alzheimer's disease. *Alzheimer Dementia* 2020;16:335-344. doi:10.1016/j.jalz.2019.08.201
56. Murray E, Ross OA, Dickson DW, et al. Neuropathologically defined subtypes of Alzheimer's disease with distinct clinical characteristics: a retrospective study. *Lancet Neurl* 2011; 10.9: 785-796. doi:10.1016/S1474
57. Mosconi L, Tsui WH, Herholz K, et al. Multicenter standardized 18F-FDG PET diagnosis of mild cognitive impairment, Alzheimer's disease, and other dementias. *J Nucl Med* 2008;49:390-398.
58. Bakker A, Krauss GL, Albert MS, et al. Reduction of hippocampal hyperactivity improves cognition in amnestic mild cognitive impairment. *Neuron* 2012;74:467-474. doi:10.1016/j.neuron.2012.03.023
59. Chételat G. Multimodal neuroimaging in Alzheimer's disease: early diagnosis, physiopathological mechanisms, and impact of lifestyle. *J Alzheimer Disease* 2018;64:S199-S211.
60. Berron D, van Westen D, Ossenkoppele R, Strandberg O, Hansson O. Medial temporal lobe connectivity and its associations with cognition in early Alzheimer's disease. *Brain* 2020;143:1233-1248.
61. Dautricourt S, de Flores R, Landeau B, et al. Longitudinal changes in hippocampal network connectivity in Alzheimer's disease. *Ann Neurol* 2021;90:391-406.
62. Lehmann M, Ghosh PM, Madison C, et al. Greater medial temporal hypometabolism and lower cortical amyloid burden in ApoE4-positive AD patients. *J Neurol Neurosurg Psychiatr* 2014;85:266. doi:10.1136/jnnp-2013-305858
63. Wolk DA, Dickerson BC, Initiative ADN, et al. Apolipoprotein E (APOE) genotype has dissociable effects on memory and attentional–executive network function in Alzheimer's disease. *Proc Natl Acad Sci* 2010;107:10256-10261.
64. Bien CG, Helmstaedter C, Elger CE. Is it really Alzheimer's disease? *J Neurol Neurosurg Psychiatry* 2001;71:416-417.
65. Teylan M, Mock C, Gauthreaux K, et al. Cognitive trajectory in mild cognitive impairment due to primary age-related tauopathy. *Brain* 2020;143:611-621. doi:10.1093/brain/awz403
66. Grothe MJ, Moscoso A, Silva-Rodríguez J, et al. Differential diagnosis of amnestic dementia patients based on an FDG-PET signature of autopsy-confirmed LATE-NC. *Alzheimers Dement* 2023;19:1234-1244.
67. Santangelo R, Masserini F, Agosta F, et al. CSF p-tau/Aβ42 ratio and brain FDG-PET may reliably detect MCI "imminent" converters to AD. *Eur J Nucl Med Mol Imaging* 2020;47:3152-3164.
68. Neuner SM, Telpoukhovskaia M, Menon V, O'Connell KMS, Hohman TJ, Kaczorowski CC. Translational approaches to understanding resilience to Alzheimer's disease. *Trends Neurosci* 2022;45(5):369-383.
69. Gefen T, Gasho K, Rademaker A, et al. Clinically concordant variations of Alzheimer pathology in aphasic versus amnestic dementia. *Brain* 2012;135:1554-1565.
70. Frings L, Hellwig S, Spehl TS, et al. Asymmetries of amyloid-β burden and neuronal dysfunction are positively correlated in Alzheimer's disease. *Brain* 2015;138:3089-3099.
71. Weise CM, Chen K, Chen Y, Kuang X, Savage CR, Reiman EM. Left lateralized cerebral glucose metabolism declines in amyloid-β positive persons with mild cognitive impairment. *Neuroimage Clin* 2018;20:286-296. doi:10.1016/j.nicl.2018.07.016
72. Zahn R, Juengling F, Bubrowski P, et al. Hemispheric asymmetries of hypometabolism associated with semantic memory impairment in Alzheimer's disease: a study using positron emission tomography with fluorodeoxyglucose-F18. *Psychiatry Res Neuroimaging* 2004;132:159-172. doi:10.1016/j.pscychresns.2004.07.006
73. Lu M, Pontecorvo MJ, Devous MD, et al. Aggregated tau measured by visual interpretation of flortaucipir positron emission tomography and the associated risk of clinical progression of mild cognitive impairment and Alzheimer disease: results from 2 phase III clinical trials. *JAMA Neurol* 2021;78:445-453.
74. Mirkin S, Albensi BC. Should artificial intelligence be used in conjunction with Neuroimaging in the diagnosis of Alzheimer's disease? *Front Aging Neurosci* 2023;15:1094233.

SUPPORTING INFORMATION

Additional supporting information can be found online in the Supporting Information section at the end of this article.

How to cite this article: Caminiti SP, De Francesco S, Tondo G, et al. FDG-PET markers of heterogeneity and different risk of progression in amnestic MCI. *Alzheimer's Dement*. 2024;20:159–172. https://doi.org/10.1002/alz.13385